Central Lancashire Online Knowledge (CLoK)

Title	Nanoclay-Directed Structure and Morphology in PVDF Electrospun Membranes
Type	Article
URL	https://clok.uclan.ac.uk/id/eprint/11295/
DOI	
Date	2014
Citation	Kelarakis, Antonios and yoon, k (2014) Nanoclay-Directed Structure and Morphology in PVDF Electrospun Membranes. Journal of Nanomaterials, 2014 (367671).
Creators	Kelarakis, Antonios and yoon, k

It is advisable to refer to the publisher's version if you intend to cite from the work.

For information about Research at UCLan please go to http://www.uclan.ac.uk/research/

Research Article

Nanoclay-Directed Structure and Morphology in PVDF Electrospun Membranes

Kyunghwan Yoon[1,2] and Antonios Kelarakis[3]

[1] *Department of Biomedical Engineering, Washington University, St. Louis, MO 63130, USA*
[2] *LG Chem, 104-1 Munji-Dong, Yuseong-Gu, Daejeon 305-380, Republic of Korea*
[3] *Centre for Materials Science, School of Forensic and Investigative Sciences, University of Central Lancashire, Preston PR1 2HE, UK*

Correspondence should be addressed to Kyunghwan Yoon; hwani92@gmail.com and Antonios Kelarakis; akelarakis@uclan.ac.uk

Academic Editor: Marta J. Krysmann

The incorporation of organically modified Lucentite nanoclay dramatically modifies the structure and morphology of the PVDF electrospun fibers. In a molecular level, the nanoclay preferentially stabilizes the all-trans conformation of the polymer chain, promoting an α to β transformation of the crystalline phase. The piezoelectric properties of the β-phase carry great promise for energy harvest applications. At a larger scale, the nanoclay facilitates the formation of highly uniform, bead-free fibers. Such an effect can be attributed to the enhanced conductivity and viscoelasticity of the PVDF-clay suspension. The homogenous distribution of the directionally aligned nanoclays imparts advanced mechanical properties to the nanofibers.

1. Introduction

Polyvinylidene fluoride (PVDF) is a widespread, low-cost engineering material that combines remarkable levels of chemical inertness, thermal resistance, mechanical strength, and flexibility [1]. The exceptional properties of PVDF are widely exploited for the preparation of high performance scaffolds and membranes for battery separators [2], western blotting [3], and ultra- and microfiltration [4]. Particular emphasis is given to the development of PVDF based piezoelectric materials, for example, materials that generate voltage in response to an external electric field [5].

Among the various approaches followed for the preparation of the nanofibrous membranes, electrospinning presents distinct advantages due to its versatility and compatibility with standard industrial processing that allows the continuous production of long nanofibers [6–8]. The morphological characteristics of the electrospun membranes critically depend upon the properties of the jet dispersion (viscosity, surface tension, conductivity, vapor pressure, and concentration) and the operational parameters (magnitude of the electric field, spinneret to collector distance, and solution feed rate) [6–8].

A large gallery of nano- and submicron particles has been incorporated into the initial polymer solution to give composite electrospun fibers with superior performance and desirable functionalities [9, 10]. With respect to PVDF based electrospun composites, systems containing yarn [11], SiO_2 [12], Ni [13], Ag [14], magnetic nanoparticles [15], carbon nanotubes (CNT) [16], and nanoclays [17] have been reported.

In this work, we demonstrate that the incorporation of organically modified Lucentite nanoclay into PVDF solutions dramatically modifies the morphology of the electrospun membranes in a multiple fashion. First, while the fibers of neat polymer suffer a dense population of bulky beads, the introduction of minor amounts of nanoclay eliminates this effect. Second, the alignment of the clay layers parallel to the fiber axis gives rise to a highly laminated superstructure. Third, the clay stabilizes the formation of the fiber-like β-crystallites at the expense of the α-spherulites of PVDF.

The defect-free nanocomposite fibers combine the desirable characteristics of the β-phase (piezoelectricity, pyroelectricity), while exhibiting advanced mechanical properties.

2. Experimental

2.1. Materials. PVDF with $M_w = 4.44 \times 10^5\,\mathrm{g\,mol^{-1}}$ (grade Kynar 761) was received from Arkema Products, and Lucentite STN grade (containing trioctyl methyl ammonium surfactants) from Co-op Chemical Co. Ltd, Japan, and dimethylformamide DMF (analytical grade) from Aldrich were used as received.

2.2. Fiber Preparation. Lucentite was first dispersed in DMF by vigorous stirring for 24 hours followed by ultrasonication for an hour. The polymer powder was added gradually to the clay suspension that was kept at 50°C for the first few hours and then at room temperature for 1 day. The suspensions were electrospun onto aluminum foil at an electric field strength of $1.7\,\mathrm{kV\,cm^{-1}}$ and a solution flow speed of $20\,\mu\mathrm{L\,min^{-1}}$. The distance between the spinneret (diameter = 0.7 mm) and the collector was kept 10 cm. In our setup, a rotating metal drum (diameter: 9 cm, rotating speed: 300 rpm) was used to collect the deposited nanofibers.

2.3. Characterization. Fiber images were taken by scanning Electron Microscopy (SEM), using a LEO 1550 equipped with a Schottky field emission gun (10 kV) and a Robinson backscatter detector. The specimens were subject to cold coating to minimize the charging effect. Transmission electron microscopy (TEM) images of the single fibers were collected by a JEOL JEM1200ex (the samples were prepared by electrospinning directly onto the copper-carbon TEM grids).

The electrospun membrane samples (length = 2.54 cm, width = 6 mm, and thickness = $90\,\mu\mathrm{m}$) were uniaxially stretched using an Instron 4442 tensile apparatus with the speed of $10\,\mathrm{mm\,min^{-1}}$ at room temperature. At least five consistent measurements were obtained for each sample.

Fourier transform Infra-red (FTIR) spectra of the samples were recorded using a Nicolet iZ10 spectrophotometer (Thermo Scientific, USA). Samples were scanned 128 times at a resolution $2\,\mathrm{cm^{-1}}$. X-ray diffraction (XRD) spectra were recorded at room temperature using a Scintag Inc. θ-θ goniometer (CuKα radiation, $\lambda = 1.54\,\text{Å}$).

An Anton-Paar Physica MCR 301 rheometer equipped with a couette geometry (diameter 27 mm) was used to measure the shear viscosity of solutions. The measurements were carried out at room temperature.

3. Results and Discussion

The XRD pattern of the neat PVDF fibers (Figure 1(a)) suggests that the polymer chains predominantly crystallize in the nonpolar α-phase as evident by the peaks (100), (020), (110), (021) at $2\theta = 18°$, 18.6°, 20.3°, and 26.9°, respectively. In contrast, the XRD pattern of the hybrid electrospun fibers
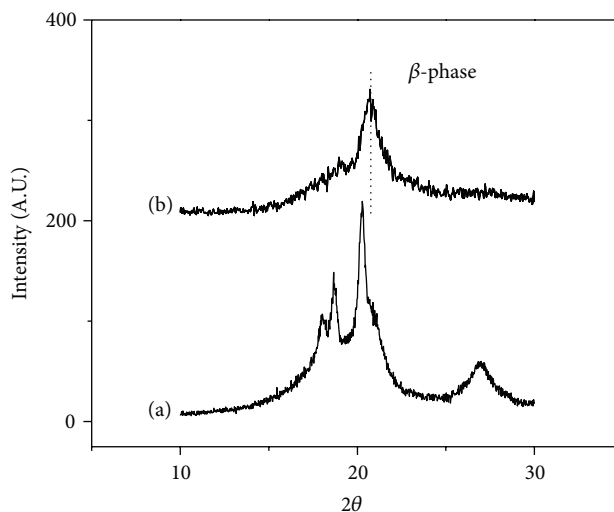

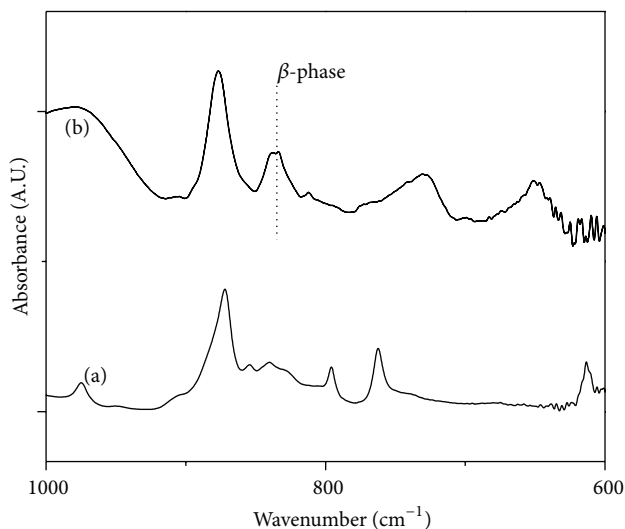Figure 1: XRD patterns of electrospun nanofibers: (a) PVDF and (b) PVDF/1.5 wt% Lucentite.

Figure 2: FTIR spectra of electrospun nanofibers: (a) PVDF and (b) PVDF/1.5 wt% Lucentite.

(containing 1 wt% of Lucentite organoclay) (Figure 1(b)) is dominated by the reflection peak $\beta(200)/\beta(110)$ at $2\theta = 20.7°$ of the orthorhombic unit cell of the β-phase [18]. The stabilization/evolution of the β-phase of PVDF in the clay hybrids is also supported by the FTIR spectra shown in Figure 2; while only the α-phase peaks centered at 763 and $796\,\mathrm{cm^{-1}}$ are present for the neat polymer fibers, the β-phase peak centered at $840\,\mathrm{cm^{-1}}$ can be clearly detected for the hybrid fibers [19].

The polymorphism of PVDF crystals stems from the symmetry and flexibility of the chains and the size proximity between the fluorine and the hydrogen atoms. Among the five crystalline phases of PVDF (α, β, γ, δ, and ε), the highest dipolar moment is observed for the β-phase, where the chains adapt their all-trans conformations and the C–H bonds are oriented perpendicular to the carbon backbone. The
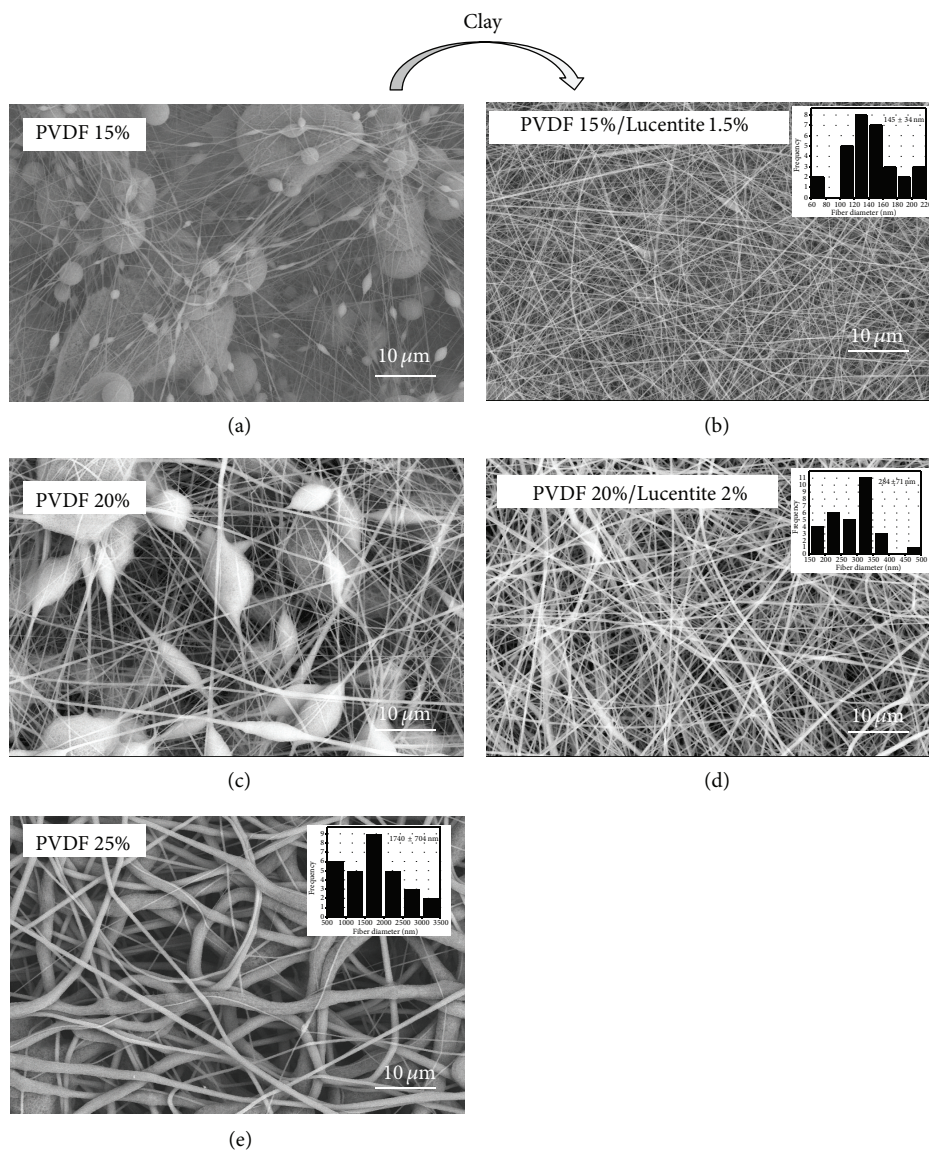
FIGURE 3: SEM images of electrospun nanofibers derived from DMF solutions containing PVDF ((a), (c), and (e)) or PVDF and Lucentite ((b), (d)) at the concentrations indicated.

technological importance of the β-phase mainly arises from its piezoelectric, pyroelectric, and ferroelectric properties, as opposed to the most common, albeit inactive, α-phase, where the chains adapt a trans-gauche-trans-gauche conformation. The piezoelectric behavior of PVDF is widely explored for energy harvest applications [6].

Accordingly, substantial efforts have been devoted in order to promote the β at the expenses of a phase. It is now well established that the β-phase of PVDF can be stabilized in the presence of various nanofillers including organically modified montmorillonite [20, 21], Lucentite clay [17, 22], functionalized graphene sheets [23], functionalized multiwall carbon nanotubes [24], and Ag nanoparticles [25]. The underlying mechanism has been attributed to the constrained nature of the polymer crystallization (in analogous to the effects seen in immiscible blends containing minor amounts

of PVDF) [26] or to the matching between the lattices of the β crystals and the inorganic filler (in analogous to the effects seen in the epitaxial crystallization on KBr) [27] or, alternatively, to the development of ion-dipole interactions between the negatively charged clay surface and the PVDF dipoles [17].

It is worth mentioning that uniaxial deformation (application of a mechanical force) and pooling (application of an electrical field), both present in electrospinning, can effectively promote an α to β transformation in PVDF crystals. In fact, electrospun nanofibers with a significant amount of β-phase have been prepared even in the absence of nucleating additives [28, 29]. The synergistic effects between electrospinning and incorporation of CNT [16] and clay [30] nanoadditives on the stabilization of the β-phase have been demonstrated.
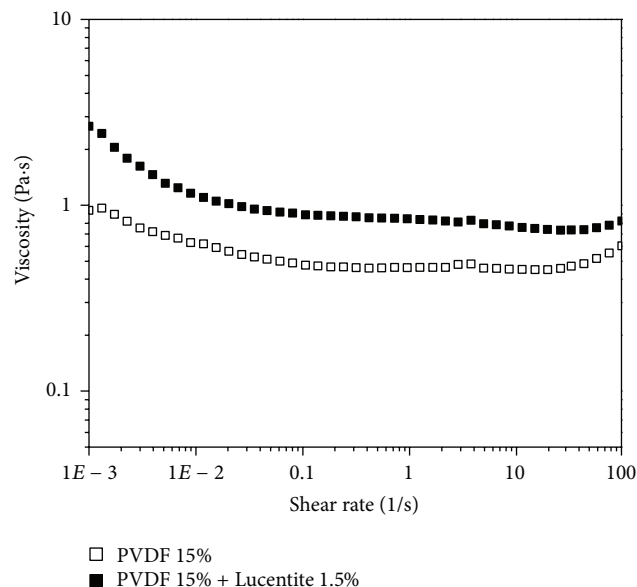
(a)

Figure 4: Shear viscosity of 15 wt% PVDF solution (open symbols) and 15 wt% PVDF/10 wt% Lucentite dispersion (close symbols) in DMF at room temperature.

A comparison between the SEM images of the neat PVDF and PVDF/nanoclay electrospun fibers (Figure 3) clearly highlights the profound impact of nanoclay inclusion on the resulting morphology. It becomes immediately apparent that incorporation of nanoclay not only eliminates the presence of beads (that thoroughly undermine the morphology of the neat PVDF fibers), but also allow the formation of ultrathin and highly uniform fibers. For example, electrospinning a 15 wt% PVDF solution in DMF leads to a material with very poor morphological characteristics (Figure 3(a)), but addition of 1.5 wt% nanoclays to, otherwise identical, solution gives rise to defect-free fibers with average diameter 145 ± 34 nm (Figure 3(b)). Moreover, electrospinning a 20 wt% PVDF solution in DMF leads to a membrane with a dense population of bulky beads (Figure 3(c)), while the corresponding fibers containing 2% nanoclay appear uniform in thickness with average diameter 284 ± 71 nm (Figure 3(d)). For reference, we note that in neat PVDF membranes we could only eliminate the bead formation by increasing the concentration up to 25 wt%, but this yielded thick fibers with average diameter 1740 ± 704 nm (Figure 3(e)).

The superior morphological characteristics of the PVDF/Lucentite electrospun fiber can be attributed to the higher viscosity and conductivity values of the polymer/clay dispersions in DMF compared to the binary polymer/DMF solutions. In Figure 4, it can be seen that the introduction of clay nanoparticles to the PVDF suspension enhances the shear viscosity. It has been supported that enhanced viscosity of the jet solution entails the presence of stronger resistance to shape deformation, facilitating the formation of uniform and smooth surfaces [7].

At the same time, addition of clay nanoparticles increases the density of the charge carriers in the system. We note that
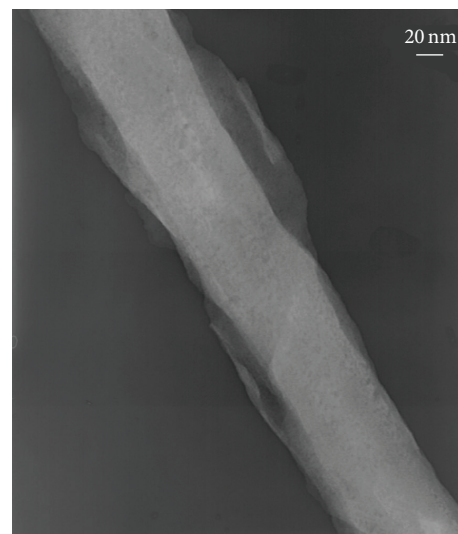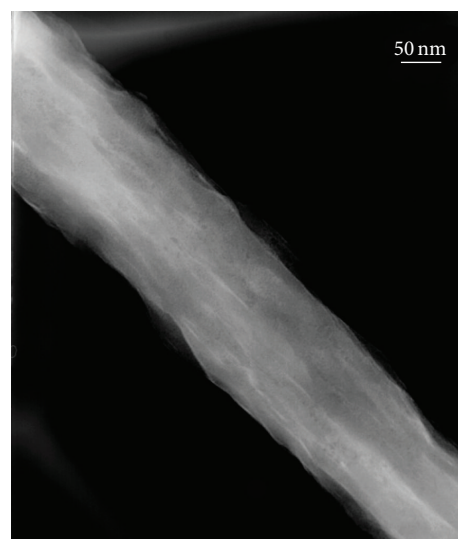
(b)

Figure 5: TEM micrographs of electrospun nanofibers: (a) PVDF and (b) PVDF/1.5 wt% Lucentite.

the cation exchange capacity, a measure of the charge density that accounts for the electric conductivity of Lucentite clays, has been estimated to be close to 0.65 mequiv/g [22]. Higher charge density in the surface of the solution jet results in stronger electrostatic repulsions that essentially reduce the surface tension forces and facilitate the formation of defect-free fibers [7].

The representative TEM images of the hybrid fiber (Figure 5) reveal the presence of well dispersed clay platelets that are oriented parallel to the axis of the fiber. The distribution of the clay platelets is uniform within the matrix with no signs of aggregation or agglomeration. The featureless low angle XRD pattern (Figure 6) collected for the nanocomposite fibers provides further evidence for the high level of intercalation/exfoliation of the clay layers (for
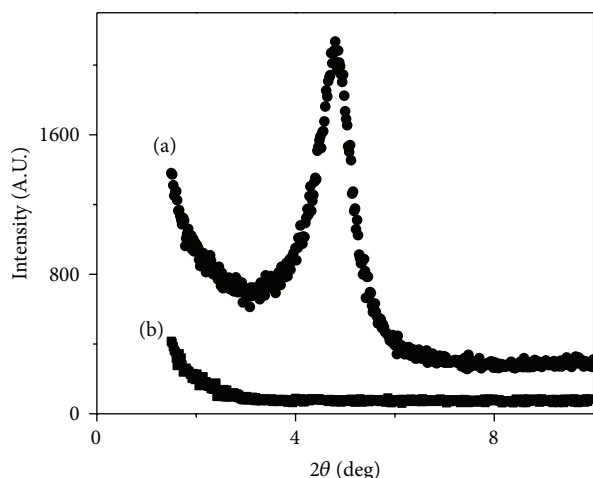
FIGURE 6: Low angle XRD patterns of (a) Lucentite clay and (b) PVDF/1.5 wt% Lucentite.

○ PVDF ● PVDF + 10% Lucentite
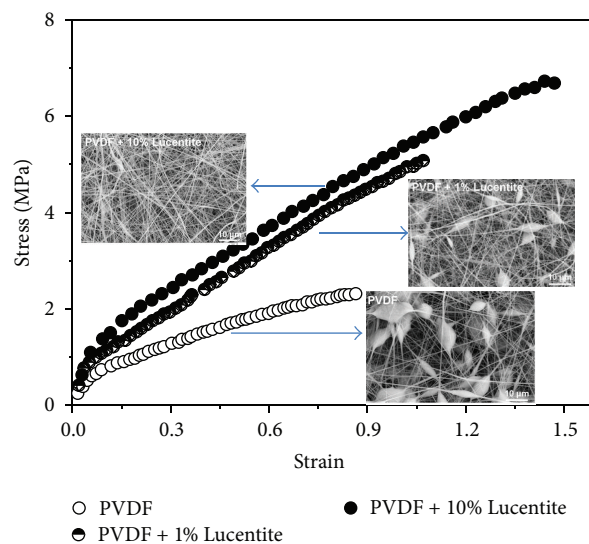◑ PVDF + 1% Lucentite

FIGURE 7: Stress-strain curves for electrospun membranes: PVDF (open circles), PVDF/1 wt% Lucentite (half-filled circles), and PVDF/10 wt% Lucentite (filled circles).

comparison the XRD pattern of the dry clay is also included in Figure 6). The directional alignment can be assigned to the strong elongation forces exerted by both the polymer crystals and the nanoadditives during electrospinning [31, 32]. The subsequent fast solvent evaporation and crystallization suppress any relaxation effects, so that both chains and particles retain largely their aligned conformations. It has been pointed out that in certain instances the embedded nanoparticles maintain a higher degree of orientation compared to the polymer matrix, as a direct consequence of their slower relaxation [33].

The nanocomposite fibers exhibit simultaneous enhancements in both mechanical strength and toughness (defined by the area under the stress-strain curves) as shown in Figure 7. In particular, the Young's modulus is 14 MPa for the neat polymeric membranes and 21 MPa for the hybrids, while the ultimate tensile strength is 2.3 MPa for the neat PVDF membranes compared to 5.1 and 6.7 MPa for the hybrids containing 1 wt% and 10 wt% Lucentite, respectively. At the same time, the elongation at break increases from 87% for the neat polymer to approximately 108% and 145% for the hybrids containing 1 wt% and 10 wt% Lucentite, respectively.

In general, incorporation of rigid particles within a polymer matrix improves the stiffness of the materials at the expense of their toughness. Substantial improvements in toughness have been reported for a limited number of clay based nanocomposite systems including PVDF [21], PVDF copolymers [19], and PVDF based blends [18]. It has been supported that dispersion of nanoparticles can facilitate new energy dissipation mechanisms, leading to advanced mechanical properties by improving the load transfer efficiency (and ultimately having a protective role against the onset of catastrophic cracking) in a manner that critically depends on the strength of the polymer-particle interactions [34]. In that sense, the superior mechanical performance of the hybrid system reported here supports the development of strong interactions between the PVDF matrix and the organically modified nanoclay.
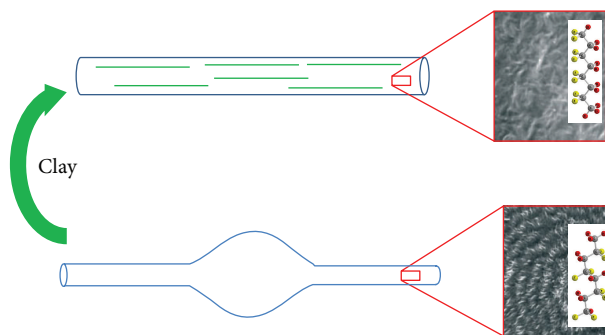
FIGURE 8: Schematic representation of the structure and morphology of neat PVDF (lower scheme) and PVDF/clay (upper scheme) electrospun membranes.

4. Conclusions

In this report, we present a unique case of nanoclay directed structure and morphology in PVDF electrospun fibers. The introduction of organically modified Lucentite to the jet solution increases the viscosity and the density of the charged carriers, facilitating the formation of uniform and bead-free fibers. At the same time, the introduction of nanoclays promotes the crystallization of the highly desirable β-phase at the expenses of the α modification of the polymer. The homogenous distribution of nanoclays and their directional alignment along to the fiber axis has a profound impact on the mechanical strength and the toughness of the fibers. A schematic representation of the dramatic structural and morphological changes induced by nanoclay is shown in Figure 8.

Conflict of Interests

The authors declare that there is no conflict of interests regarding the publication of this paper.

References

[1] J. S. Humphreys and R. Amin-Sanayei, *Vinylidene Fluoride Polymers*, John Wiley & Sons, New York, NY, USA, 2002.

[2] P. Arora and Z. Zhang, "Battery separators," *Chemical Reviews*, vol. 104, no. 10, pp. 4419–4462, 2004.

[3] E. Cho, C. Kim, J.-K. Kook et al., "Fabrication of electrospun PVDF nanofiber membrane for western blot with high sensitivity," *Journal of Membrane Science*, vol. 389, pp. 349–354, 2011.

[4] J. F. Hester, P. Banerjee, Y.-Y. Won, A. Akthakul, M. H. Acar, and A. M. Mayes, "ATRP of amphiphilic graft copolymers based on PVDF and their use as membrane additives," *Macromolecules*, vol. 35, no. 20, pp. 7652–7661, 2002.

[5] C. Sun, J. Shi, D. J. Bayerl, and X. Wang, "PVDF microbelts for harvesting energy from respiration," *Energy & Environmental Science*, vol. 4, no. 11, pp. 4508–4512, 2011.

[6] D. H. Reneker and I. Chun, "Nanometre diameter fibres of polymer, produced by electrospinning," *Nanotechnology*, vol. 7, no. 3, pp. 216–223, 1996.

[7] D. Li and Y. Xia, "Electrospinning of nanofibers: reinventing the wheel?" *Advanced Materials*, vol. 16, no. 14, pp. 1151–1170, 2004.

[8] A. Greiner and J. H. Wendorff, "Electrospinning: a fascinating method for the preparation of ultrathin fibers," *Angewandte Chemie*, vol. 46, no. 30, pp. 5670–5703, 2007.

[9] Z.-M. Huang, Y.-Z. Zhang, M. Kotaki, and S. Ramakrishna, "A review on polymer nanofibers by electrospinning and their applications in nanocomposites," *Composites Science and Technology*, vol. 63, no. 15, pp. 2223–2253, 2003.

[10] D. Li, Y. Wang, and Y. Xia, "Electrospinning of polymeric and ceramic nanofibers as uniaxially aligned arrays," *Nano Letters*, vol. 3, no. 8, pp. 1167–1171, 2003.

[11] A. Baji, Y. W. Mai, X. Du, and S.-C. Wong, "Improved tensile strength and ferroelectric phase content of self-assembled polyvinylidene fluoride fiber yarns," *Macromolecular Materials and Engineering*, vol. 297, no. 3, pp. 209–213, 2012.

[12] Y. J. Kim, C. H. Ahn, M. B. Lee, and M. S. Choi, "Characteristics of electrospun PVDF/SiO$_2$ composite nanofiber membranes as polymer electrolyte," *Materials Chemistry and Physics*, vol. 127, no. 1-2, pp. 137–142, 2011.

[13] F. A. Sheikh, T. Cantu, J. Macossay, and H. Kim, "Fabrication of poly(vinylidene fluoride) (PVDF) nanofibers containing nickel nanoparticles as future energy server materials," *Science of Advanced Materials*, vol. 3, no. 2, pp. 216–222, 2011.

[14] J. Yuan, J. Geng, Z. C. Xing, J. Shen, I.-K. Kang, and H. Byun, "Electrospinning of antibacterial poly(vinylidene fluoride) nanofibers containing silver nanoparticles," *Journal of Applied Polymer Science*, vol. 116, no. 2, pp. 668–672, 2010.

[15] J. S. Andrew and D. R. Clarke, "Enhanced ferroelectric phase content of polyvinylidene difluoride fibers with the addition of magnetic nanoparticles," *Langmuir*, vol. 24, no. 16, pp. 8435–8438, 2008.

[16] S. Huang, W. A. Yee, W. C. Tjiu et al., "Electrospinning of polyvinylidene difluoride with carbon nanotubes: synergistic effects of extensional force and interfacial interaction on crystalline structures," *Langmuir*, vol. 24, no. 23, pp. 13621–13626, 2008.

[17] L. Yu and P. Cebe, "Crystal polymorphism in electrospun composite nanofibers of poly(vinylidene fluoride) with nanoclay," *Polymer*, vol. 50, no. 9, pp. 2133–2141, 2009.

[18] A. Kelarakis, E. P. Giannelis, and K. Yoon, "Structure-properties relationships in clay nanocomposites based on PVDF/(ethylene-vinyl acetate) copolymer blends," *Polymer*, vol. 48, no. 26, pp. 7567–7572, 2007.

[19] A. Kelarakis, S. Hayrapetyan, S. Ansari, J. Fang, L. Estevez, and E. P. Giannelis, "Clay nanocomposites based on poly(vinylidene fluoride-co-hexafluoropropylene): structure and properties," *Polymer*, vol. 51, no. 2, pp. 469–474, 2010.

[20] L. Priya and J. P. Jog, "Poly(vinylidene fluoride)/clay nanocomposites prepared by melt intercalation: crystallization and dynamic mechanical behavior studies," *Journal of Polymer Science B*, vol. 40, no. 15, pp. 1682–1689, 2002.

[21] D. Shah, P. Maiti, E. Gunn et al., "Dramatic enhancements in toughness of polyvinylidene fluoride nanocomposites via nanoclay-directed crystal structure and morphology," *Advanced Materials*, vol. 16, no. 14, pp. 1173–1177, 2004.

[22] J. Buckley, P. Cebe, D. Cherdack et al., "Nanocomposites of poly(vinylidene fluoride) with organically modified silicate," *Polymer*, vol. 47, no. 7, pp. 2411–2422, 2006.

[23] S. Ansari and E. P. Giannelis, "Functionalized graphene sheet-poly(vinylidene fluoride) conductive nanocomposites," *Journal of Polymer Science B*, vol. 47, no. 9, pp. 888–897, 2009.

[24] C. Xing, L. Zhao, J. You, W. Dong, X. Cao, and Y. Li, "Impact of ionic liquid-modified multiwalled carbon nanotubes on the crystallization behavior of poly(vinylidene fluoride)," *The Journal of Physical Chemistry B*, vol. 116, no. 28, pp. 8312–8320, 2012.

[25] S. Manna, S. K. Batabyal, and A. K. Nandi, "Preparation and characterization of silver-poly(vinylidene fluoride) nanocomposites: formation of piezoelectric polymorph of poly(vinylidene fluoride)," *The Journal of Physical Chemistry B*, vol. 110, no. 25, pp. 12318–12326, 2006.

[26] X. Yang, X. Kong, S. Tan, G. Li, W. Ling, and E. Zhou, "Spatially-confined crystallization of poly(vinylidene fluoride)," *Polymer International*, vol. 49, no. 11, pp. 1525–1528, 2000.

[27] A. J. Lovinger, "Crystallization of the β phase of poly(vinylidene fluoride) from the melt," *Polymer*, vol. 22, no. 3, pp. 412–413, 1981.

[28] J. C. McGrath and I. M. Ward, "High effective draw as a route to increased stiffness and electrical response in poly(vinylidene fluoride)," *Polymer*, vol. 21, no. 8, pp. 855–857, 1980.

[29] K. C. Satyanarayana and K. Bolton, "Molecular dynamics simulations of α- to β-poly(vinylidene fluoride) phase change by stretching and poling," *Polymer*, vol. 53, no. 14, pp. 2927–2934, 2012.

[30] Y. L. Liu, Y. Li, J. T. Xu, and Z. Q. Fan, "Cooperative effect of electrospinning and nanoclay on formation of polar crystalline phases in poly(vinylidene fluoride)," *ACS Applied Materials & Interfaces*, vol. 2, no. 6, pp. 1759–1768, 2010.

[31] H. Fong, W. Liu, C.-S. Wang, and R. A. Vaia, "Generation of electrospun fibers of nylon 6 and nylon 6-montmorillonite nanocomposite," *Polymer*, vol. 43, no. 3, pp. 775–780, 2002.

[32] Y. Ji, B. Li, S. Ge, J. C. Sokolov, and M. H. Rafailovich, "Structure and nanomechanical characterization of electrospun PS/clay nanocomposite fibers," *Langmuir*, vol. 22, no. 3, pp. 1321–1328, 2006.

[33] J. J. Ge, H. Hou, Q. Li et al., "Assembly of well-aligned multiwalled carbon nanotubes in confined polyacrylonitrile

environments: electrospun composite nanofiber sheets," *Journal of the American Chemical Society*, vol. 126, no. 48, pp. 15754–15761, 2004.

[34] A. Kelarakis, K. Yoon, I. Sics, R. H. Somani, B. S. Hsiao, and B. Chu, "Uniaxial deformation of an elastomer nanocomposite containing modified carbon nanofibers by in situ synchrotron X-ray diffraction," *Polymer*, vol. 46, no. 14, pp. 5103–5117, 2005.